JCEC
THE JOURNAL OF ENGINEERING AND EXACT SCIENCES

OPEN ACCESS

The Journal of Engineering and Exact Sciences – jCEC, Vol. 10 N. 05 (2024)
journal homepage: https://periodicos.ufv.br/jcec
eISSN: 2527-1075
ISSN: 2446-9416

Complexes of a piperazine based macrocycle as Cu-Zn SOD biomimetic: approach by constants determination

Complexos de um macrociclo baseado em piperazina como biomimético Cu-Zn SOD: abordagem pela determinação de constantes

Complejos de un macrociclo basado en piperazina como biomimético de la Cu-Zn SOD: un acercamiento por determinación de constantes

Article Info:
Article history: Received 2024-03-03 / Accepted 2024-06-05 / Available online 2024-07-15
doi: 10.18540/jcecvl10iss5pp19230

Armando Ferrer Serrano
ORCID: https://orcid.org/0000-0002-6849-0232
Departamento de Química, Facultad de Ciencias Naturales y Exactas, Universidad de Oriente, Cuba
Departamento de Química Orgânica, Instituto de Química, Universidade Federal da Bahía, Salvador de Bahía, Bahía, Brazil
E-mail: aferrers@uo.edu.cu
armandoferrerserrano@gmail.com
Ilena Alicia García del Toro
ORCID: https://orcid.org/0009-0005-6444-4131
Delegación Territorial del CITMA (Ministerio de Ciencia Tecnología y Medio Ambiente), Santiago de Cuba, Cuba
E-mail: ilena@citmascu.gob.cu

Abstract
Obtaining new compounds capable of catalyzing the dismutation reaction of the superoxide anion carried out by the enzyme Cu,Zn-SOD has become a topic of great interest. In the present work, the study of a ligand with a piperazine fragment and its Cu(II) and Zn(II) complexes is introduced. The protonation constants of the ligand, the stability constants of the complex species un with equivalent of Cu(II) and Zn(II), forming both mononuclear and heterobinuclear species, in the presence and absence of histidine as secondary ligand were determined. For all cases, species distribution diagrams were obtained, from which the spectra in the visible region of the species of greatest interest were obtained. As an approach to the Cu,Zn-SOD system, the formation of quaternary species formed between these ions, the main ligand and histidine as a secondary ligand, was verified, which could be used as mimetics of said enzyme. Some theoretical studies were carried out to support this study.
Keywords: Protonation. Complex. Macrocycle. Biomimetic. Cu,Zn-SOD.

Resumo
A obtenção de novos compostos capazes de catalisar a reação de dismutação do ânion superóxido realizada pela enzima Cu,Zn-SOD tornou-se tema de grande interesse. No presente trabalho é introduzido o estudo de um ligante com fragmento de piperazina e seus complexos Cu(II) e Zn(II). Foram determinadas as constantes de protonação do ligante, as constantes de estabilidade das espécies complexas un com equivalentes de Cu(II) e Zn(II), formando espécies mononucleares e heterobinucleares, na presença e ausência de histidina como ligante secundário. Para todos os casos

foram obtidos diagramas de distribuição de espécies, a partir dos quais foram obtidos os espectros na região do visível das espécies de maior interesse. Como abordagem ao sistema Cu,Zn-SOD, foi verificada a formação de espécies quaternárias formadas entre esses íons, o ligante principal e a histidina como ligante secundário, que poderiam ser utilizadas como miméticos da referida enzima. Alguns estudos teóricos foram realizados para embasar este estudo.
Palavras-chave: Protonação. Complexo. Macrociclo. Biomimético. Cu,Zn-SOD.

Resumen
La obtención de nuevos compuestos capaces de catalizar la reacción de dismutación del anión superóxido realizada por el enzima Cu,Zn-SOD se ha convertido en un tema de gran interés. En el presente trabajo se introduce el estudio de un ligando con un fragmento piperazina y sus complejos de Cu(II) y Zn(II). Se determinaron las constantes de protonación del ligando, las constantes de estabilidad de las especies complejas un con equivalente de Cu(II) y Zn(II), formando tanto especies mononucleares como heterobinucleares, en presencia y ausencia de histidina como ligando secundario. Para todos los casos se obtuvieron los diagramas de distribución de especies, a partir de los cuales se obtuvieron los espectros en la región visible, de las especies de mayor interés. Como un acercamiento al sistema Cu,Zn-SOD, se comprobó la formación de especies cuaternarias formadas entre estos iones, el ligando principal y la histidina como ligando secundario, las que pudieran ser empleadas como miméticos de dicho enzima. Algunos estudios teóricos se realizaron para apoyar este estudio.
Palabras clave: Protonación. Complejo. Macrociclo. Biomimética. Cu,Zn-SOD.

Nomenclature
L: 5,9,17,21-tetraaza-1,13(1,4)-dipiperazina-7,19(1,3)-dibenzenacyclotetracosaphane-6,8,18,20-tetraone.
Hys (histidine). Although the histidine symbol is His, in this publication Hys is used to distinguish this amino acid in nomenclature of coordination compounds.

1. Introduction.

The chemistry of metal ions in biological systems is largely solution chemistry, and therefore coordination chemistry. Among the variety of biomolecules that can act as ligands, proteins stand out especially. The study of their metal complexes, metalloproteins, currently constitutes the most important part of Bioinorganic Chemistry. The chemical behavior of a metal ion in a metalloprotein should not be essentially different from that in its simpler complexes. However, the macromolecular nature of the protein ligand may specifically limit or modulate the reactivity of the resulting complex. (Vallet, 2003; Nazif, 2021)

The metalloenzyme Cu-Zn Superoxide Dismutase catalyzes the dismutation reaction of the superoxide anion. Under normal conditions, in a healthy organism, $O_2^{\bullet-}$ free radicals are trapped by this enzyme but when there is an overproduction of radicals or poor work in the defense mechanisms, their control becomes a problem. Therefore, the preparation of small molecules capable of mimicking the active site of Cu,Zn-SOD has become a topic of great interest. (Vallet, 2003; Verdejo, 2007; Serbest, 2021; Zengin, 2023)

On the other hand, macrocycles are compounds with diverse dimensions, shapes and conformations that present environments capable of coordinating metal ions. These molecules, from the point of view of coordination chemistry, can house one or more metal centers in their cavities, this being one of the aspects that enriches the Chemistry of macrocyclic ligand complexes and allows them to be used as mimetics of various metalloenzymes. (Taut, 2023; Vallet, 2003; Jung, 2021)

Continuing the study of this type of bio-complexes in biological fluids is extremely

complicated, due to the influence of many factors, such as: the pH of the medium, the possible interactions with other electron-rich biomolecules, the different behavior it may have. the protein bound to the metal outside its usual environment (possible denaturation), among others. Macrocyclic ligands offer the possibility of simulating, approximately, the coordination environment around the metal ion, including the great stability that occurs when coordinating (macrocycle effect) with respect to the union with monodentate ligands. (Cragg, 2010; Bregier-Jarzebwska, 2019; Kubik, 2017)

That is why this research is aimed at simulating, through the use of low molecular weight macromolecular ligands, the structure and functioning of metalloenzymes such as Cu-Zn Superoxide Dismutase (Cu,Zn-SOD). Therefore, determining the formation constants in solution of quaternary complexes of a macrocyclic amino/amide ligand with Cu^{2+}, Zn^{2+} and histidine could bring us closer to the most similar combination to the enzyme mentioned above and the appropriate conditions in solution for its formation.

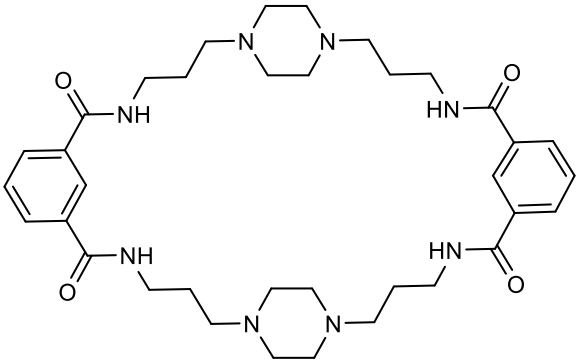

Chart 1 - Structure of the ligand L.

2. Materials and methods.

All reagents used in this work were purchased from commercial sources, except the isophthalic ester with N-hydroxysuccinimide, which was synthesized (Hernández, 2014).

2.1 Synthesis.

Isophthalic acid (5.00 g, 30.1 mmol) and N-hydroxysuccinimide (6.93 g, 60.2 mmol) are dissolved in dry THF at 0 °C. Upon obtaining a clear solution, DCC (12.48 g, 60.5 mmol) dissolved in anhydrous THF is added drop by drop and the resulting solution is stirred at 0-5°C for 3h. The dicyclohexylurea formed is filtered and the filtrate is concentrated to dryness. The crude product is recrystallized from 2-propanol to obtain the pure product. Yield: 51.1%; M.P: 186-189ºC; white solid; ^{1}H NMR (500 MHz, DMSO-d6): δ(ppm) 8.63(1H, s); 8.51(2H,d); 7.94(1H,t), 2.89(8H,m).

The ligand L, used to perform the potentiometric measurements, was synthesized according to described procedures (Verdejo, 2007; Algarra, 2009). In a three-mouth ball, 100 mL of DME is added. Separately, in addition funnels, 0.29 mL (1.42 mmol) of 3,3'-(piperazine-1,4-diyl)bis(propan-1-amine) are placed in one of them and in the other 0.50 g (1.39 mmol) of the isophthalic ester with N-hydroxysuccinimide previously synthesized (Both dissolved in DME). It is added dropwise into the receiving solvent placed on the balloon, under constant stirring and in an ice bath. The mixture is kept under stirring for 12 h, then the solid is removed by vacuum filtration, washed with DME and recrystallized from 2-propanol. Yield: 64 %; white solid; M.P: 147-148 ºC; ^{1}H NMR (500MHz, CD_3OD): δ(ppm) 7,88 (2H,s, Ar-H); 7,52 (2H,d, Ar-H); 7,42 (4H,d, Ar-H); 8,20 (4H,s, amide); 3,15 (8H,t, -CH_2-amide); 1,81 (8H,m, -CH_2-); 2,95 (8H,t, -CH_2-amine); 2,29 (8H,t, -CH_2- piperazine).

2.2 Potentiometric measurements.

The potentiometric titrations were carried out at 298.1 ± 0.1 K using NaCl 0.1 M as supporting electrolyte. The experimental procedure (burette, potentiometer, cell, stirrer, microcomputer, etc.) has been fully described elsewhere (Verdejo, 2007; Algarra, 2009). The acquisition of the emf data was performed with the computer program Crison Capture. The reference electrode was an Ag–AgCl electrode in saturated KCl solution. The glass electrode was calibrated as a hydrogen-ion concentration probe by titration of previously standardized amounts of HCl with CO_2-free NaOH solutions and the equiv. point determined by the Gran's method (Gran, 1952), which gives the standard potential, E°, and the ionic product of water [pKw = 13.78]. The computer program HYPERQUAD was used to calculate the protonation and stability constants, and the HySS program was used to obtain the distribution diagrams (Gans, 1996).

Next, the ligand was titrated with the Cu (II) and Zn (II) ion respectively, in a 1:1 M:L ratio. Then, the macrocyclic ligand was titrated with Cu (II) and Zn (II) simultaneously in the ratio Cu:Zn:L 1:1:1. Furthermore, prior to the evaluation of the quaternary system, the evaluations of the M:L:Hys systems were carried out in a 1:1:1 ratio. Finally, the macrocyclic ligand was assessed with Cu (II), Zn (II) and Histidine in the ratio Cu:Zn:L:Hys 1:1:1:1. In all cases, ionic strength of NaCl 0.15 mol·dm^{-3} was used.

The pH range investigated was 2.0–11.0. The different titration curves for each system (at least two) were treated either as a single set or as separated curves without significant variations in the values of the stability constants. Finally, the sets of data were merged together and treated simultaneously to give the final stability constants. The electronic spectra were obtained in a Reyleigh UV-2601 Spectrophotometer.

3. Results and discussion.

3.1 Ligand synthesis.

The synthesis of the ligand was carried out following the high dilution method described in the literature to obtain macrocycles (Yu, 2013). It is known that the more diluted the medium is, the reaction will be directed more toward the formation of the macrocycle than toward polymerization. However, it is possible to obtain small macrocycles of type [1+1] and at the same time, larger ones, [2+2]. Although in this case, the semi-rigidity of the piperazine fragment would help, through conformational control, the prevalence of the largest macrocycle [2+2] (Chart 2).

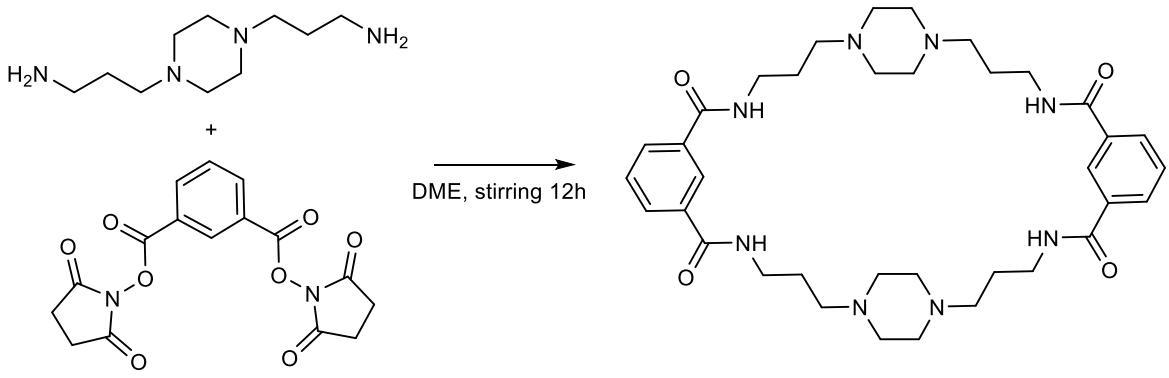

Chart 2 – Scheme of synthesis of the ligand L.

A white compound was obtained, that appeared pure in thin layer chromatography. The ^{1}HNMR spectrum showed all the expected signals (see experimental part: Materials and Methods). In addition, others appear, such as the corresponding water retained in the structure (something common in pseudopeptidic compounds or with several amide groups), as a peak is noted at 3.30

ppm that indicates water when deuterated methanol is used. Some additional singlets appear too, and can be attributed to intramolecular interactions of amine and amide groups (Demarque, 2017). It is interesting to see how spatially the symmetry expected for this type of molecule is lost due to the multiple existing intramolecular interactions, which can be made more complex by the presence of some type of occluded solvent (Figure 1) (Valls, 2022; Omolara, 2018).

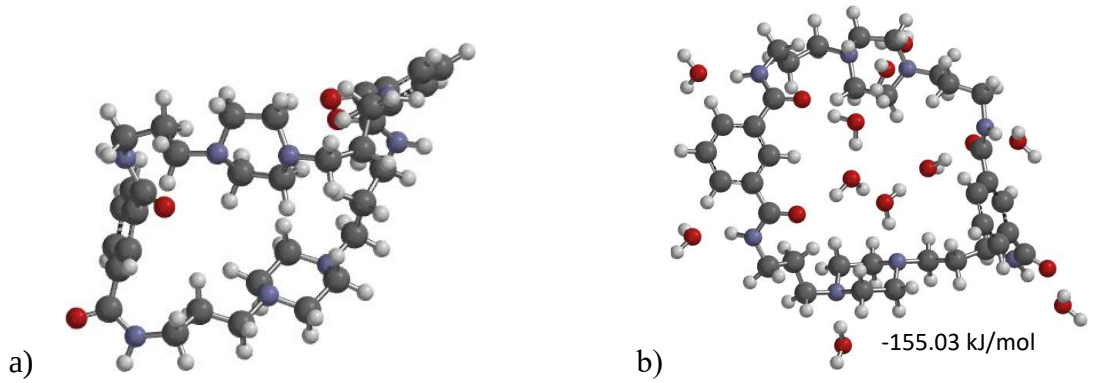

Figure 1 – Asymmetrical 3D structure of L. a) Intramolecular interactions (modelled in vaccum). b) Possible occlusion of water molecules due to H bonds. (3D Draw by software Spartan 08 version 1.2.0). (Omolara, 2018)

3.2 Ligand protonation.

The ligand presents four measurable protonation steps in the pH range of study. Four protonation constants were found as well as, two unusual deprotonations.

The protonation constants detected are slightly lower than what was previously reported by this same team for similar ligands (Hernández, 2014; Alves de Silva, 2017; Martí, 2012; Ferrer, 2022). In this case, the ionic strength used was a little higher (0.15M) with the aim of seeking a greater similarity to the ionic strength of the human organism. Some papers show that Log K decreases with increasing ionic strength (Al-Rashdi, 2018). The decrease in the values of the successive protonation constants can be rationalized based on the electrostatic repulsion created by the consecutive addition of positive charges to the already positive charged specie (Ferrer, 2022). In this case, the first two protonations could go to different piperazine fragments in order to minimize the electrostatic repulsions between both positive charge densities. The log K values for the third and fourth protonation are lower since these must occur in nitrogen atoms adjacent to those already protonated, thus increasing the Coulombic repulsion.

The literature reports higher values of protonation constants for tertiary amines (Algarra, 2009), an aspect that suggests that in this case there is some additional effect that could be causing lower values. One reason may be that the proximity between the tertiary amino groups causes additional proton stabilization of the protonated species and the exit of the proton becomes more difficult (Figure 2).

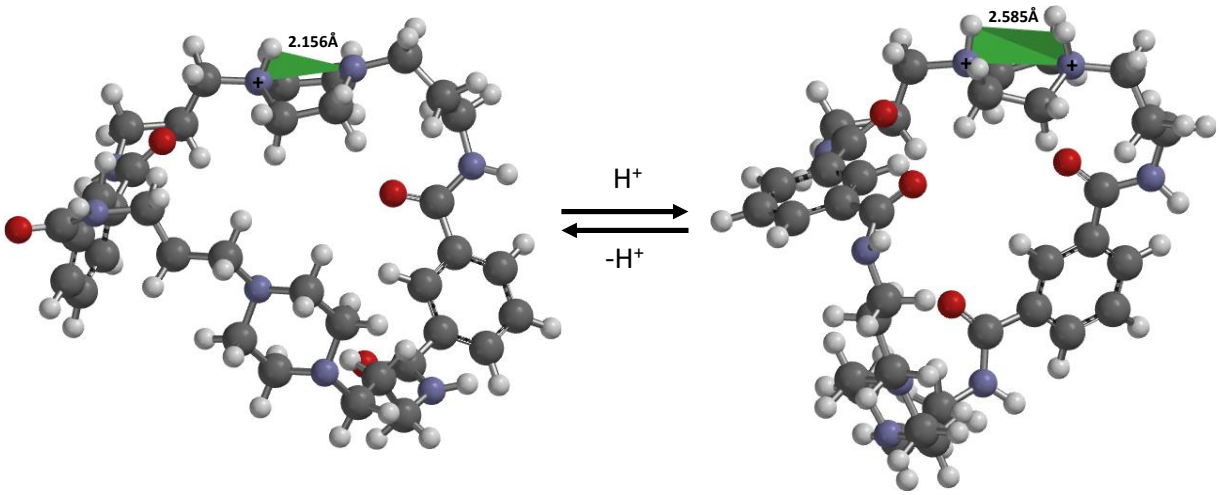

Figure 2 - Intramolecular Hydrogen bond in pyperazine fragment for LH^+ and LH_2^{2+} (modeled by software Spartan 08 version 1.2.0). (Omolara, 2018)

The acidity constant obtained may be attributed either to the deprotonation of two of the amide nitrogen atoms or to the hydrolysis of molecules of water bound by hydrogen bonds to both amide groups of one isophthalic moiety. The first of these options is less probable because the deprotonation of the amide group itself is a very endergonic process and can take place only if this negative contribution is more than compensated by a very exothermic interaction (Fabrizzi, 2008). The second option can be supported by reports of crystalline structures of other compounds including isophtalic fragments, in which one molecule of water is attached by hydrogen bonds to both amide nitrogen atoms (Brooks, 2006; Bernier, 2009). This phenomenon was also observed by this team of researchers in a ligand of a similar nature (Ferrer, 2022). Table 1 shows all cumulative and stepwise constants determined for this ligand.

Table 1 – Logarithms of the cumulative and stepwise basicity and acidity constants determined in 0.15 M NaCl at 298.1 ± 0.1 K.

Species[a]	Log β	Equilibrium (K)	Log K
LH	7.04(2) [b]	[LH]/[L][H]	7.04(2)
LH_2	12.51(2)	$[LH_2]/[LH][H]$	5.47(2)
LH_3	17.16(2)	$[LH_3]/[LH_2][H]$	4.65(2)
LH_4	20.51(2)	$[LH_4]/[LH_3][H]$	3.35(2)
LH_{-1}	-8.99 (2)	$[LH_{-1}]/[L][OH]$	-8.99(2)
LH_{-2}	-19.38(2)	$[LH_{-2}]/[LH_{-1}][OH]$	-10.39(2)

[a] Charges omitted. [b] Values in parentheses are the error in the last significant figure.

Figure 3 shows the species distribution diagram in 0.15 M NaCl for this ligand, constructed from the values of the determined cumulative constants. It is possible to observe that the free ligand exists at pH 7 values, indicating its basic nature, being predominant at pH 8.00 with 82.4% relative abundance.

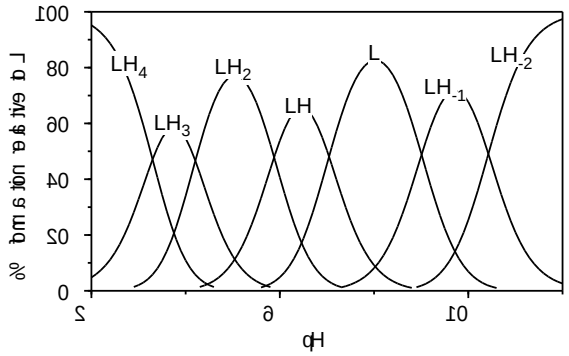

Figure 3 - Distribution diagram for the species of L in 0.15 M NaCl at 298.1 K.

3.2 Mononuclear LM complex systems.

Taking into account the previous protonation study and the data on the constants of copper (II) and zinc (II) hydroxocomplexes reported in the literature (Plyasunova, 1997), the formation constants of the complexes were proposed and calculated. After manual adjustment and several refinements in the program, the results presented in Table 2 were obtained.

It is possible to notice the easy entry of a Cu (II) cation into the interior of the macrocyclic cavity due to the stability of the resulting species $[CuL]^{2+}$ (log K = 7.42). The same occurs for $[ZnL]^{2+}$ complexes, with a slightly lower value of log K = 6.30. However, these both values are below those reported for polyazamacrocyclic ligands, whose log K values are essentially between 13 and 21 (Basallote, 2006; Castillo, 2014). This could be due, to a certain extent, to the steric hindrance imposed by the carbon atoms associated with the tertiary nitrogen atoms of the piperazine fragment.

Table 2 – Logarithms of the formation constants for mononuclear complexes of the ligand determined in 0.15 M NaCl at 298.1 ± 0.1 K at M:L ratio 1:1.

Species[a]	Cu(II)		Zn(II)		Equilibrium (K)
	Log β	Log K	Log β	Log K	
MLH_2	17.28(2)	4.49(2)	17.01(3)	4.68(3)	$[MLH_2]/[MLH][H]$
MLH	12.79(2)	5.37(2)	12.33(2)	6.03(2)	[MLH]/[ML][H]
ML	7.42(2)	7.42(2)	6.30(3)	6.30(3)	[ML]/[L][M]
MLH_{-1}	1.84(2)	-5.58(2)	.1.31(3)	-7.61(3)	$[MLH_{-1}]/[ML][OH]$
MLH_{-2}	-4.08(2)	-5.92(2)	-9.56(3)	-8.25(3)	$[MLH_{-2}]/[MLH_{-1}][OH]$
MLH_{-3}	-11.6(2)	-7.52(2)	-18.2(3)	-8.65(3)	$[MLH_{-3}]/[MLH_{-2}][OH]$
MLH_{-4}			-28.49(3)	-10.28(3)	$[MLH_{-4}]/[MLH_{-3}][OH]$

[a] Charges omitted. [b] Values in parentheses are the error in the last significant figure.

It is also interesting to observe the deprotonation phenomenon in the complexes that are formed at basic pH values (see species distribution diagram, Figure 4, where they have been represented interchangeably as MLH_{-x}). However, it is likely that in the case of copper II complexes, the first species with this formula (MLH_{-1}) corresponds to the entry of an OH group into the Cu coordination sphere, replacing a water molecule. While in the case of Zn complexes, this occurs in

the MLH_{-1} and MLH_{-2} complexes. In this way the complexes that form at higher pH values can be attributed to deprotonations of the amide groups (Anagnostopoulos, 1995).

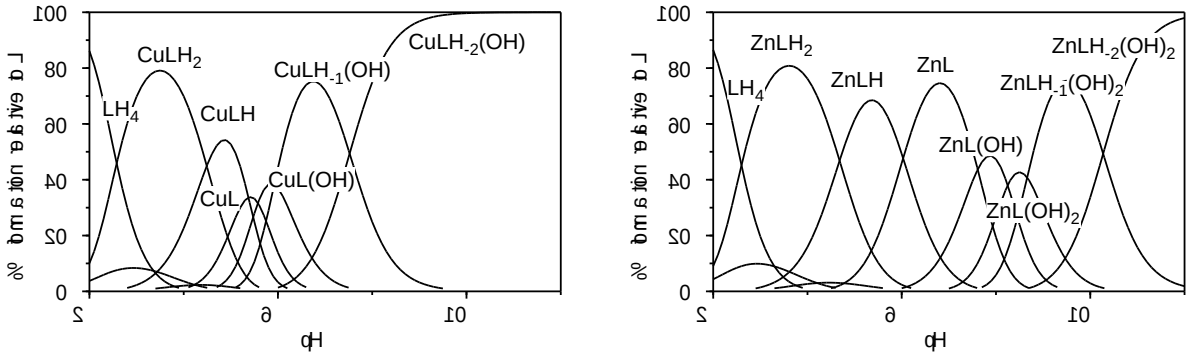

Figure 4 - Species distribution diagrams for the different Cu(II) and Zn(II) mononuclear complexes at M:L molar ratio 1:1.

3.3 Cu-Zn Hetero-dinuclear coordination systems.

The studied ligand presents two areas that offer similar coordination environments, and can not only form mononuclear complexes as we saw previously. This is why we proceeded to determine the formation constants of heterobinuclear complexes with both cations under study, seeking an approach to the Cu,Zn-SOD enzyme. Thus, the formation constants of this type of complexes are shown in the following Table. It is interesting to observe that the entry of a second cation to this ligand is favored in both cases, be it the entry of Zn(II) to the mononuclear copper complex or Cu(II) to the mononuclear Zn complex (Table 3).

In the same way as described in the previous section, it is likely that the first species that appear with the hypothetical MLH_{-x} structure correspond to the entry of OH into the coordination sphere of both Cu(II) and Zn(II). While those that appear at higher pH values promote the deprotonation of the amide groups.

Table 3 – Logarithms of the formation constants for hetero-dinuclear Cu-Zn complexes with ligand L, determined in 0.15 M NaCl at 298.1 ± 0.1 K at Cu:Zn:L, molar ratio 1:1:1.

Species[a]	Log β	Log K	Equilibrium (K)
CuZnL	11.25(3) [b]	11.25(3)	[CuZnL]/[Cu][Zn][L]
		3.83 (3)	[CuZnL]/[CuL][Zn]
		4.95(3)	[CuZnL]/[Cu][ZnL]
$CuZnLH_{-1}$	4.96(1)	-6.29(1)	$[CuZnLH_{-1}]$/[CuZnLH][OH]
$CuZnLH_{-2}$	0.14(2)	-4.82(2)	$[CuZnLH_{-2}]$/[$CuZnLH_{-1}$][OH]
$CuZnLH_{-3}$	-7.44(2)	-7.58(2)	$[CuZnLH_{-3}]$/[$CuZnLH_{-2}$][OH]
$CuZnLH_{-4}$	-15.51(2)	-8.07(2)	$[CuZnLH_{-4}]$/[$CuZnLH_{-3}$][OH]

[a] Charges omitted. [b] Values in parentheses are the error in the last significant figure.

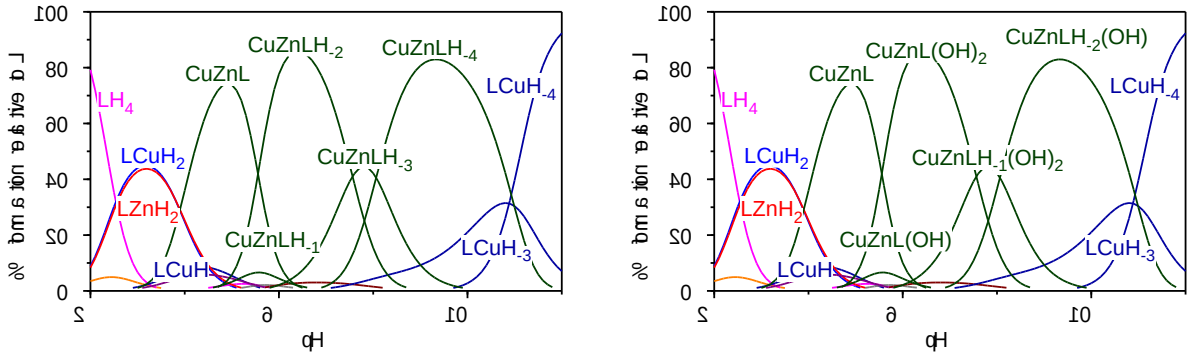

Figure 5 - Species distribution diagrams for the different hetero-dinuclear Cu-Zn complexes with ligand L, Cu:Zn:L molar ratio 1:1:1.

3.4 Systems with a high level of complexity: Cu/Zn/L/Histidine.

Up to this point, we have heterobinuclear complexes that harbor two different cations, Cu(II) and Zn(II), similar to the SOD enzyme that we want to "mimic." However, the structures described in the literature indicate that there is an imidazole bridge between both cations (Spagnolo, 2004; Strange, 2006; Strange, 2012), perhaps coming from a histidine residue (Figure 6, PDB). This suggests that it has an important influence on the biological function of the enzyme, which is why it is necessary to study systems that contain both cations and histidine as a secondary ligand.

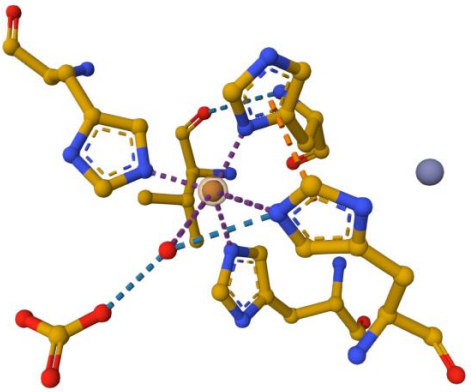

Figure 6 - Active site of Cu-Zn SOD, reported in Protein Data Bank, adapted from 4B3E (Spagnolo, 2012).

Before studying the Cu/Zn/Histidine system; It is necessary to understand the interaction of each metal with histidine independently as a basis for a better understanding. The results of the titrations and subsequent data processing are shown in the Table 4.

In this system where a secondary ligand (histidine) appears, the Log β values indicate how favoured the formation of tertiary complexes is. It was also observed that the entry of this secondary ligand histidine is favoured, a little more for the mononuclear Cu(II) complexes (with Log K = 11.15) than for their Zn(II) homologues (with Log K = 5.02). This suggests that the binding of histidine to the copper (II) cation is perhaps more favoured by the affinity of the nitrogen atoms for this ion. As in the previous sections, there is both the possibility of deprotonation occurring and the entry of hydroxyl groups. However, taking into account that two ligands coexist with the possibility of being deprotonated from pH 7, the deprotonation hypothesis seems to be the most indicated, so far.

Table 4 – Logarithms of the cumulative and stepwise constants for mononuclear complexes of Cu (II) and Zn (II) with the ligand, in the presence of histidine (Hys), determined in 0.15 M NaCl at 298.1 ± 0.1 K at M:L:Hys molar ratio 1:1:1.

Species[a]	Cu(II)		Zn(II)		Equilibrium (K)
	Log β	Log K	Log β	Log K	
$MLH_2(Hys)$	28.37(2)	4.59(2)	24.40(3)	5.49(3)	$[MLH_2(Hys)]/[MLH(Hys)][H]$
MLH(Hys)	23.78(2)	5.21(2)	18.61(2)	7.29(2)	[MLH(Hys)]/[ML(Hys)][H]
ML(Hys)	18.57(2)	11.15(2)	11.32(3)	5.02(3)	[ML(Hys)]/[ML][Hys]
$MLH_{-1}(Hys)$	11.50(2)	-7.07(2)	3.60(3)	-7.72(3)	$[MLH_{-1}(Hys)]/[ML(Hys)][OH]$
$MLH_{-2}(Hys)$	1.93(2)	-9.57(2)	-4.50(3)	-8.15(3)	$[MLH_{-2}(Hys)]/[MLH_{-1}(Hys)][OH]$
$MLH_{-3}(Hys)$			-14.3(3)	-9.77(3)	$[MLH_{-3}(Hys)]/[MLH_{-2}(Hys)][OH]$

[a] Charges omitted. [b] Values in parentheses are the error in the last significant figure.

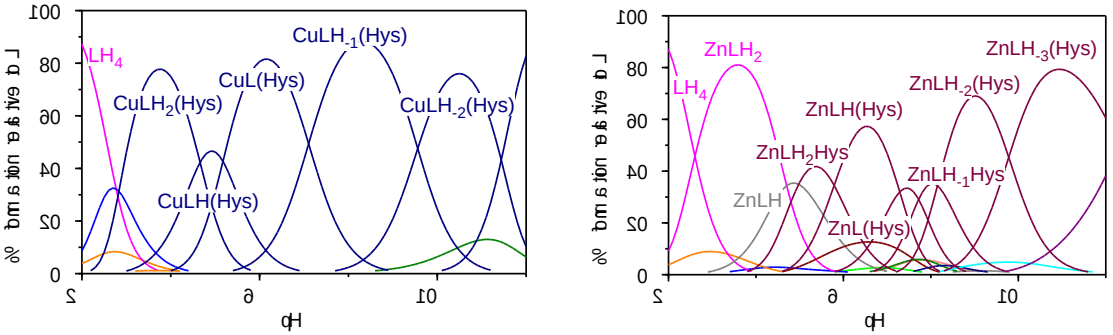

Figure 7 - Species distribution diagrams for mononuclear complexes of Cu (II) and Zn (II) with the ligand, in the presence of histidine (Hys).

Once the formation of mononuclear complexes with histidine as a secondary ligand had been explored, the constants of the tertiary heterobinuclear complexes were determined, giving the results shown in the following table.

Table 5 – Logarithms of the cumulative and stepwise constants of Cu(II) and Zn(II) complex formation with the ligand L and histidine as secondary ligand, ratio M1:M2:L:Hys 1:1:1:1,determined in 0.15 M NaCl at 298.1 ± 0.1 K.

Species [a]	Log β [b]	Log K	Equilibria
$[CuZnLH_2(Hys)]$	32.58(5)	4.79(5)	$[CuZnLH(Hys)] + H^+ = [CuZnLH_2(Hys)]$
[CuZnLH(Hys)]	27.39(6)	4.67(6)	$[CuZnLHis] + H^+ = [CuZnLH(Hys)]$
[CuZnL(Hys)]	23.12(5)	11.67(5)	[CuZnL] + Hys = [CuZnL(Hys)]
$[CuZnH_{-2}L(Hys)]$	11.92(5)	-11.20(5)	$[CuZnL(Hys)] + 2OH^- = [CuZnH_{-2}L(Hys)]$
$[CuZnH_{-3}L(Hys)]$	5.58(6)	-6.34(6)	$[CuZnH_{-2}L(Hys)] + OH^- = [CuZnH_{-3}L(Hys)]$
$[CuZnH_{-5}L(Hys)]$	-10.77(4)	-16.35(4)	$[CuZnH_{-3}L(Hys)] + 2OH^- = [CuZnH_{-5}L(Hys)]$
$[CuZnH_{-6}L(Hys)]$	-19.22(4)	-8.45(4)	$[CuZnH_{-5}L(Hys)] + OH^- = [CuZnH_{-6}L(Hys)]$

[a] Charges omitted. [b] Values in parentheses are the error in the last significant figure.

This time the entry of the auxiliary ligand histidine is even more favoured (Log K= 11.67) than when only one cation is found within the designed macrocycle. The reasons seem to be clear: an even greater coordination environment, where the imidazole ring could be placed, in some of the arrangements, as a bridge between both cations. An aspect that would bring this system closer to the desired biomimetic system. For an even more complex system from the point of view of the equilibria that can occur as the pH changes, it is difficult to propose structures of protonated or deprotonated species. However, it is interesting to note that complex species containing Cu, Zn and the auxiliary ligand histidine (regardless of the degree of protonation or deprotonation), begin to form from approximately pH 4, to values greater than 12 (Figure 8). This is of great importance since the mimetic point of view, since dismutation reactions of the superoxide anion could be explored in a wide range of pH.

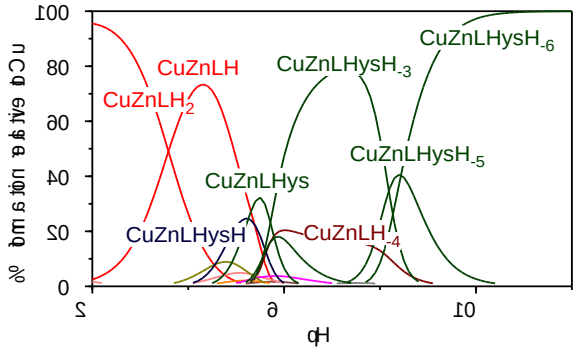

Figure 8 - Species distribution diagrams of Cu(II) and Zn(II) complex formation with the ligand L and histidine as secondary ligand, ratio M1:M2:L:Hys 1:1:1:1,determined in 0.15 M NaCl at 298.1 ± 0.1 K.

*3.5 Exploring about the structure by Spectroscopy UV-visible and theoretical approximations using Spartan 08***.**

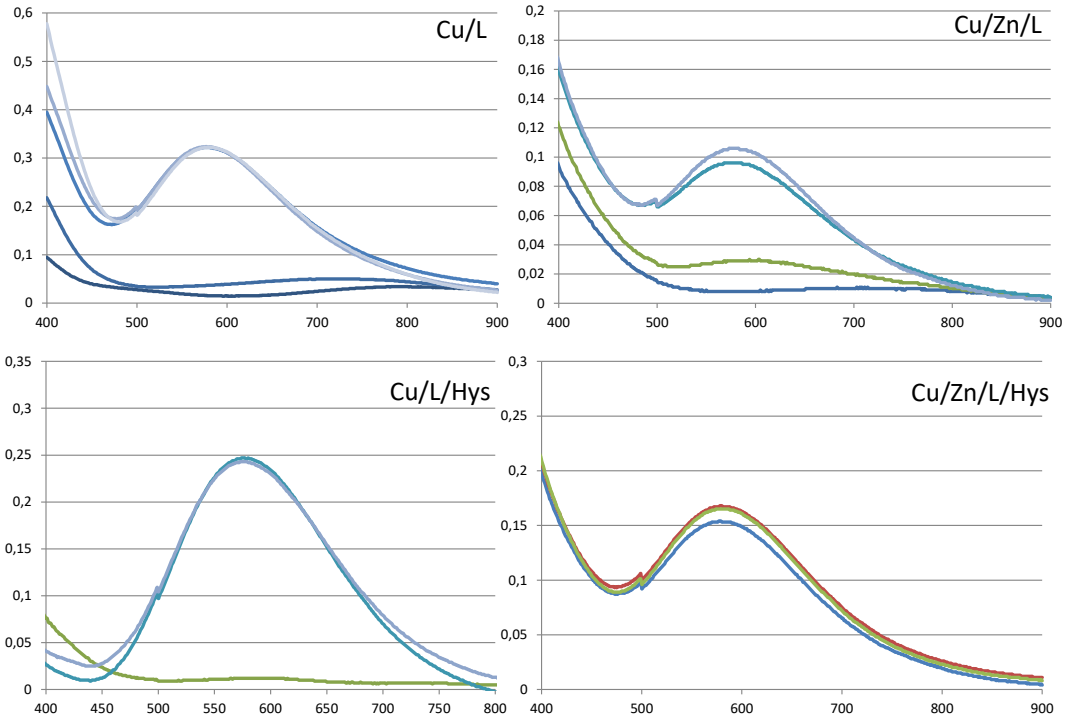

Figure 9 – UV-visible spectra of the different system that contains Cu(II) vs pH.

Figure 9 shows UV-visible spectra of all complexes that contains Cu(II), recorded at different values of pH (based on the corresponding species distribution diagrams). It stands out in this analysis that all the spectra recorded from pH 6, regardless of the system studied, show a single wavelength, located around 577-580nm (Table 6). Everything indicates that the coordination environment around the Cu(II) cation hardly changes from one species to another (pH = 6-12), without being significantly affected by the secondary ligand present in each case (H_2O, OH, histidine), nor by deprotonation processes. This aspect is also relevant for its possible use as a mimetic.

Table 6 – Some wavelengths vs pH for the different systems studied.

pH	λ_{max} (nm)			
	Cu/L	Cu/Zn/L	Cu/L/Hys	Cu/Zn/L/Hys
4	708	-	708	-
6	578	577	575	579
8	577	577	-	579
9	577	-	578	580

It is possible that the geometry of the coordination site around Cu(II) is a square-based pyramid with some distortion, assuming that this cation can have the well-known Jahn Teller effect and adopts coordination number 5 (Figure 10). The literature describes numerous complex compounds that show bands between 550 and 60nm exhibiting this type of geometry (Prenesti, 2006).

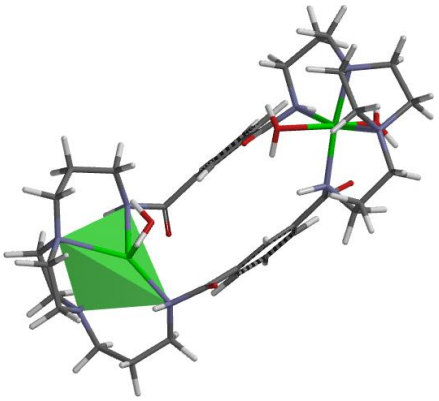

Figure 10 – Structure optimized using Spartan 08 showing a distortion of a square pyramidal for Cu(II) center (bottom), forced by piperazine fragment, while Zn(II) is a perfect octahedral.

On the other hand, various coordination environments of heterobinuclear complexes were modeled, seeking an estimate of the distance between both coordination centers and its relationship with the stabilization energy of the resulting complex, in order to have an idea of which was the best structural proposal (Figure 11). The criterion to follow was to place the aromatic ring or the piperazine fragment as a spacer, as well as an intermediate structure between both cases. As a result, a lower energy was obtained for the coordination environment that contains the aromatic ring as a spacer, which provides a certain rigidity to the complex and sets an inter-cationic distance. Nevertheless, it is necessary to take into account that the piperazine fragment induces greater stability by injecting a bimacrocyclic effect around the coordinated cation, because there are two secondary amines linking each metal (Figure 10).

This detail could be sterically important in the process of histidine approaching a heterobinuclear complex of Cu(II) and Zn(II), with this semirigid macrocyclic ligand, causing entry preferentially through the copper II cation. An exploration carried out in the Spartan 08 software shows a close-up of the imidazole ring of histidine to the hydroxyl bonded as a secondary ligand of

the copper II ion (modeling of [CuZnL(OH)] + Hys). Then, a ligand substitution could occur, leaving the histidine linked to the copper II cation. Finally, the resulting tertiary complex would increase its stability due to possible supramolecular interactions of the aliphatic chain of the amino acid through the carboxyl of aminoacid with the hydroxyl group (or water) coordinated to the zinc cation (Figure 12).

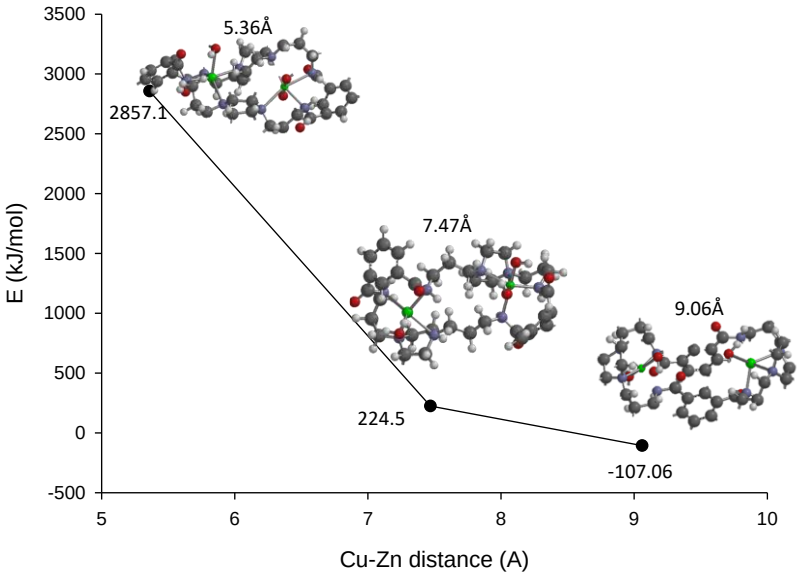

Figure 11 – Different coordination environments for heterobinuclear complexes: energy vs Cu-Zn distance.

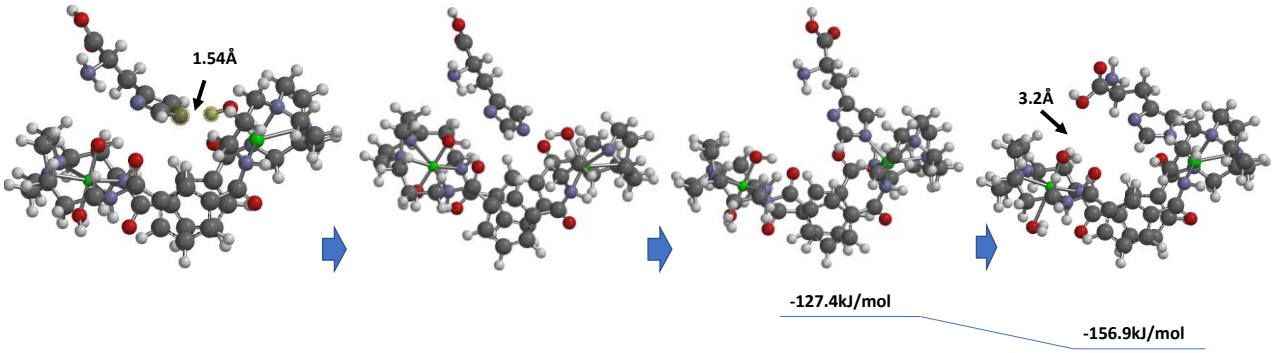

Figure 12 – Hypothetical scheme of histidine binding to Cu-Zn complex. Some energies and hydrogen bond are included.

4. Conclusions.

In this work, it was shown that this macrocyclic ligand is able to form complexes heterobinuclear with copper and zinc, as well as binding an additional ligand such as histidine. The species distribution diagrams of these tertiary heterobinuclear complexes indicate their formation from pH 4 onwards, independently of the deprotonation or gain of hydroxyl groups. This means that it can be used, in principle, as a biomimetic of Cu,Zn-SOD. Mononuclear complexes of both Zn and Cu were also studied, with and without the presence of histidine, showing the ability of both cations to bind this secondary ligand by forming tertiary complexes. The comparison between the stability constants shows a greater affinity of histidine for copper II, with respect to zinc II. The spectra recorded in the visible region indicate that the coordination environment around the Cu(II) cation is

the same in almost all the complexes formed above pH 4, for all the systems studied that contain this cation. This indicates the high stability imposed by the piperazine fragment of the ligand. Finally, some theoretical studies at a basic level help to understand possible coordination environments, distances between metal centers, binding modes with the secondary ligand histidine, etc. In this way, this system can be proposed as biomimetic once the relevant reactions have been tested.

Acknowledgements.

A. Ferrer wants to thank the Research Group Supramolecular and Sustainable Chemistry and Universitat Jaume I (Spain) for the financial and laboratory supports. Specially we want to thanks S. V. Luis, head of this group for the transmitted knowledge and friendship. Also, A. Ferrer thanks Universidade Federal da Bahía, Brazil for the support as visitor professor.

References

Al-Rashdi, A., Naggar, A.H., Farghaly, O.A., Mauof, H.A., Ekshiba, A.A., (2018). Potentiometric determination of stability constants of sulphathiazole and glycine- metal complexes., *Am. J. Analytical Chem.*, 9, 99-112. eISSN: 2156-8278.

Algarra, A., Basallote, M.G., Castillo, C.E., Clares, M.P., Ferrer, A., García-España, E., Llinares, J.M., Máñez, M.A., & Soriano, C. (2009). Geometric Isomerism in Pentacoordinate Cu^{2+} Complexes: Equilibrium, Kinetic, and Density Functional Theory Studies Reveal the Existence of Equilibrium between Square Pyramidal and Trigonal Bipyramidal Forms for a Tren-Derived Ligand., *Inorganic Chemistry*, 48, 902-914. https://doi.org/10.1021/ic8013078

Alves Da Silva, J., Felcman, J., Ramalho Mercê, A.L., Sálvio Mangrich, A., Lopes, R.S.C, & Cerqueira Lopes, C. (2003). Study of binary and ternary complexes of copper (II) with some polyamines and adenosine 5′ triphosphate., *Inorg. Chim. Acta*, 356, 155. https://doi.org/10.1016/S0020-1693(03)00462-6

Anagnostopoulos, A., Hadjispyrou, S., (1995). Effects of Mixed-Ligand Complex Formation on Deprotonation of Amide Groups in N-benzoylglycine and N-(4-aminobenzoyl) glycine. *Journal of Inorganic Biochemistry*, 57, 279-286. ISSN:1873-3344

Basallote, M.G., Doménech, A., Ferrer, A., García-España, E., Llinares, J. M., Máñez, M. A., Soriano, C., Verdejo, B., (2006), Synthesis and Cu(II) coordination of two new hexaamines containing alternated propylenic and ethylenic chains: Kinetic studies on pH-driven metal ion slippage movements. *Inorganica Chimica Acta*, 359, 2004-2014. https://doi:10.1016/j.ica.2006.01.030

Bernier, N., Carvalho, S., Li, F., Delgado, R., & Félix, V. (2009). Anion recognition by a macrobicycle based on a tetraoxadiaza macrocycle and an isophthalamide head unit., *J. Org. Chem.*, 74, 4819. https://doi.org/10.1021/jo9005798

Bregier-Jarzebwska, R., Stegient-Nowicka, J., Hoffmann, S. K., Gąsowska, A., & Łomozik, L. (2019). Studies of ternary complexes formed in the biocoordination systems including copper(II) ions, polyamines and L-lysine., *Polyhedron*, 173, 114137. https://doi.org/10.1016/j.poly.2019.114137

Brooks, S.J., Gale, P., & Light, M.E., (2006). Network formation by a pyrrole functionalized isophthalamide., *Cryst. Eng. Comm.*, 8, 877. https://doi.org/10.1039/B612524G

Castillo, C.E., Algarra, A.G., Ferrer, A., Máñez, M.A., Basallote, M.G., Clares, M.P., Soriano, C., Albelda, M.T., García-España, E., (2014), Equilibrium and kinetics studies on bibrachial lariat aza-crown/Cu(II) systems reveal different behavior associated with small changes in the structure. *Inorganica Chimica Acta*, 417, 246-257. https://doi.org/10.1016/j.ica.2013.12.020

Cragg, P.J., (2010). *Supramolecular Chemistry: From Biological inspiration to Biomedical applications*, Springer Dordrecht Heildelberg, London.

Demarque, D.P., Merten, Ch., (2017). Intra- vs. intermolecular hydrogen bonding: Solvent-dependent conformational preferences of a common supramolecular binding motif from 1H-NMR and VCD spectra. *Chem. Eur. J.*, http://dx.doi.org/10.1002/chem.201703643

Fabbizzi, L., (2008). Chapter: Fluorescent Sensors for and with Transition Metals, in *Transition Metals in Supramolecular Chemistry*, (Ed.: J. P. Sauvage), John Wiley & Sons, New York.

Ferrer, A., Hernández, Y., (2022). Selective union of ATP vs ADP to an amino/amide macrocycle and its Cu^{2+} complexes: potentiometric, spectrophotometric and theoretical approximations, *Journal of Engineering and Exact Sciences*., 08(06), 1-19. DOI:10.18540/jcecvl8iss6pp14571-01i. eISSN: 2527-1075

Gans, P., Sabatini, A., & Vacca. A. (1996). Investigation of equilibria in solution. Determination of equilibrium constants with the HYPERQUAD suite of programs., *Talanta*, 43, 1739. https://doi.org/10.1016/0039-9140(96)01958-3

Gran, G., (1952). Determination of the Equivalence Point in Potentiometric Titrations. Part II., *Analyst*, 77, 661. https://doi.org/10.1039/AN9527700661

Hernández, Y., Ferrer, A., & Blanco, M. (2014). Nuevo macrociclo tipo amino/amida: síntesis, caracterización y constantes de acidez/ basicidad. *Revista Cubana de Química*, XXVI, 32. ISSN 2224-5421.

Jung, S-M., Lee, J., & Song, W-J. (2021). Design of artificial metalloenzymes with multiple inorganic elements: The more the merrier., *J. Inorg. Biochem.*, 223, 111552. https://doi.org/10.1016/j.jinorgbio.2021.111552

Kubik, S., (2017). Anion recognition in aqueous media by cyclopeptides and other synthetic receptors., *Acc. Chem. Res.*, 50(11), 2870-2878. https://doi.org/10.1021/acs.accounts.7b00458

Marti, I., Ferrer, A., Escorihuela, J., Burguete, M.I., & Luis, S.V. (2012). Copper (II) Complexes of Bis(amino amide) Ligands: Effect of Changes in the Amino Acid Residue, *Dalton Trans.*, 41, 6764. https://doi.org/10.1039/C2DT12459A

Nazif, M., Sahin, E., & Erbas-Cakmak, S., (2021). Bio-inspired molecular machines and their biological applications. *Coord. Chem. Rev.*, 443, 214039. https://doi.org/10.1016/J.CCR.2021.214039

Omolara, A., (2018). Computational modelling Procedures for Geometry Optimization, Kinetic and Thermodynamic Calculations using Spartan Software - A Review. *Archives of Organic and Inorganic Chemical Sciences.*, 1(5), 122-125. http://doi.org/10.32474/AOICS.2018.01.000123

Plyasunova, N.V., Wang, M., Zhang, Y., Muhammed, M., (1997). Critical evaluation of thermodynamics of complex formation of metal ions in aqueous solutions II. Hydrolysis and hydroxo-complexes of Cu^{2+} at 298.15 K, *Hydrometallurgy*, 45(1-2), 37-51. ISSN:1879-1158

Prenesti, E., Daniele, P.G., Berto, S., Toso S., (2006). Spectrum–structure correlation for visible absorption spectra of copper(II) complexes showing axial co-ordination in aqueous solution. *Polyhedron*, 25, 2815–2823. doi:10.1016/j.poly.2006.04.026

Serbest, K., Dural, T., Emirik, M., Zengin, A., Faiz, Ö., (2021). Heteroligand bivalent transition metal complexes with an azo-oxime ligand and 1,10-phenanthroline: Synthesis, spectroscopy, thermal analysis, DFT calculations and SOD-mimetic activities. *Journal of Molecular Structure*, 1229, 129579. https://doi.org/10.1016/j.molstruc.2020.129579

Spagnolo, L., Toro, I., D'Orazio, M., O'Neill, P., Pedersen, J.Z., Carugo, O., Rotilio, G., Battistoni, A., Djinovic-Carugo, K., (2004). Unique Features of the sodC-encoded Superoxide Dismutase from Mycobacterium tuberculosis, a Fully Functional Copper-containing Enzyme Lacking Zinc in the Active Site. *Journal of Biological Chemistry*, 279: 33447-33455. https://doi.org/10.1074/jbc.M404699200

Strange, R.W., Antonyuk, S.V., Hough, M.A., Doucette, P.A., Valentine, J.S., Hasnain, S.S., (2006). Variable Metallation of Human Superoxide Dismutase: Atomic Resolution Crystal Structures

of Cu-Zn, Zn-Zn and as-Isolated Wild-Type Enzymes. *J Mol Biol*, 356, 1152. https://doi.org/10.1016/j.jmb.2005.11.081

Strange, R.W., Hough, M.A., Antonyuk, S.V., Hasnain, S.S., (2012). Structural Evidence for a Copper-Bound Carbonate Intermediate in the Peroxidase and Dismutase Activities of Superoxide Dismutase. *PLoS One*, 7: 44811. https://doi.org/10.1371/journal.pone.0044811

Taut, J., Chambron, J.C., Kersting, B., (2023). Fifty Years of Inorganic Biomimetic Chemistry: From the Complexation of Single Metal Cations to Polynuclear Metal Complexes by Multidentate Thiolate Ligands. *Eur. J. Inorg. Chem*., 26, e202200739. https://doi.org/10.1002/ejic.202200739

Vallet, M., Faus, J., García-España, E., Moratal, J., (2003). *Introducción a la Química Bioinorgánica*, Ed. Síntesis, Madrid.

Valls, A, Burguete, M.I., Kuret, L., Altava, B., & Luis, S. V. (2022). Open chain pseudopeptides as hydrogelators with reversible and dynamic responsiveness to pH, temperature and sonication as vehicles for controlled drug delivery., *J. Mol. Liquids*, 348, 118051. https://doi.org/10.1016/j.molliq.2021.118051

Verdejo, B., Ferrer, A., Blasco, S., Castillo, C. E., González, J., Latorre, J., Máñez, M.A., García Basallote, M., Soriano, C., & García-España, E. (2007). Hydrogen and Copper Ion-Induced Molecular Reorganizations in Scorpionand-like Ligands. A Potentiometric, Mechanistic, and Solid-State Study., *Inorganic Chemistry*, 46, 5707-5719. https://doi.org/10.1021/ic700643n

Yu, X., Sun, D., (2013). Macrocyclic Drugs and Synthetic Methodologies toward Macrocycles. *Molecules*, 18, 6230–6268.

Zengin, A., Serbest, K., Emirik, M., Özil, M., Mentece, E., Faiz, Ö., (2023). Binuclear Cu(II), Ni(II) and Zn(II) complexes of hydrazone Schiff bases: Synthesis, spectroscopy, DFT calculations, and SOD mimetic activity. *Journal of Molecular Structure*, 1278, 134926. https://doi.org/10.1016/j.molstruc.2023.134926

Zhang, Y., Muhammed, M., (2001). Critical evaluation of thermodynamics of complex formation of metal ions in aqueous solutions. *Hydrometallurgy*, 60, 215. ISSN:1879-1158